JOURNAL OF GUIDANCE, CONTROL, AND DYNAMICS
Vol. 26, No. 1, January–February 2003

Fault Tolerant Flight Control

Meir Pachter* and Yih-Shiun Huang†
U.S. Air Force Institute of Technology, Wright–Patterson Air Force Base, Ohio 45433-7765

A fault tolerant flight control system is developed. The three-module controller consists of 1) a system identification module, 2) an adaptive parameter estimate smoother, and 3) a proportional and integral compensator for tracking control. Specifically, the classical Kalman filter for linear control systems is extended so that the control system's state and loop gain are jointly estimated online, and an adaptive smoother is developed to reduce automatically the fluctuations in the gain estimate and bursting. The output of the system identification and gain smoother modules is used to adjust continuously the tracking controller's gain to compensate for a possible reduction in the loop gain due to control surface area loss caused by failure or battle damage.

I. Introduction

SYSTEM identification allows us to acquire the estimates of the plant's parameters from measurements on the system's inputs and outputs using algorithms and software, but without adding extra hardware, that is, sensors or actuators.[1,2] Unfortunately, system identification, which entails the estimation of all of the (linear) plant's parameters, resides in the realm of nonlinear filtering. Moreover, system identification for adaptive and reconfigurable flight control requires 1) the accurate and reliable estimation of the aircraft's stability and control derivatives with online operation, 2) accurate and reliable estimation at low signal-to-noise ratio (SNR), 3) the use of a small sample, and 4) no human intervention.

In this paper, a rigorous, and, therefore, unbiased real-time estimate of the parameters of the control matrix and a reliable predicted estimation error covariance are obtained without using state rate measurements.[3–5] The classical Kalman filter theory for linear control systems is extended, and the control system's state and loop gain are jointly estimated. A simplified (single-input) version of this problem is addressed, and an algorithm for the estimation of a single-input flight control system's critical loop gain parameter is developed.[6,7] The latter might change abruptly as a result of control surface area loss caused by failure or battle damage.

An adaptive smoother is developed to reduce automatically the fluctuations in the parameter estimate caused by measurement noise and by instances of poor excitation before the use of the parameter estimate in the controller. As we move from window to window, the fluctuations in the parameter estimate are further exacerbated by the presence of modeling error. Hence, the parameter estimate smoother, which precludes the onset of "bursting," is important.

Thus, an indirect adaptive and reconfigurable control system is developed. The controller consists of three modules: 1) a system identification module, 2) an adaptive parameter estimate smoother, and 3) a proportional and integral compensator for tracking control.

The architecture of an indirect adaptive and reconfigurable flight control system that incorporates the online loop gain identification algorithm, adaptive loop gain estimate smoother, and tracking controller developed in this paper, is shown in Fig. 1. The plant model is representative of the longitudinal dynamics of an F-16 class aircraft. The pilot inputs a pitch rate command q_c, which is the reference signal for the adaptive controller. The commanded input is passed through a low-pass prefilter and into a proportional and integral (PI) controller designed to yield good tracking performance. The identification algorithm, that is, the modified Kalman filter, is fed with the noise-corrupted measurements of the states of the plant, α_m and q_m, and the input to the plant δ_e. The $\hat{\alpha}$, $\hat{q}$, and $\hat{K}$ estimates of α, q, and K, respectively, are provided by the modified Kalman filter/system identification module at each time sample. This information is fed to an adaptive smoother module that calculates a smoothed estimate $\hat{K}_s$ of $\hat{K}$. The filtered loop gain estimate $\hat{K}_s$ is fed back into the forward path after the summing junction of the states and reference signal r, but before the actuator, to compensate for the changing open-loop gain K due to plant failure, that is, a loss in control surface area.

The paper is organized as follows. The system identification algorithm for loop gain estimation is provided in Sec. II. The adaptive loop gain smoothing algorithm is developed in Sec. III. The design of the linear tracking controller and the aircraft model are discussed in Sec. IV. The simulation results are presented in Sec. V followed by conclusions in Sec. VI.

II. System Identification Algorithm

A Kalman filter is a data processing algorithm that uses all available data, such as plant model, initial conditions, and statistical descriptions of any biases, measurement noise, or process noise.[8] This information is fed into the propagate/update algorithm, which then optimally derives an estimated value for the system's state in a way that minimizes estimation error variance. The rigorous Kalman filtering paradigm for linear systems can also be extended to provide an estimate of the control matrix B. Our main result is the following system identification algorithm, a preliminary version of which was presented in Ref. 6.

Theorem: Consider the following linear estimation problem. The linear dynamic system is

$$x_{k+1} = Ax_k + Kbu_k + \Gamma w_k \tag{1}$$

$$E\left(w_k w_k^T\right) = Q, \qquad k = 0, 1, \ldots, N-1 \tag{2}$$

the prior information is

$$x_0 \in N\left(\bar{x}_0, P_{0_{xx}}\right), \qquad K \in N\left(K_0, p_{0_{KK}}\right)$$

the output signal is

$$y_{k+1} = Cx_{k+1} \tag{3}$$

and the observation equation is

$$z_{k+1} = y_{k+1} + v_{k+1}, \qquad E\left(v_{k+1} v_{k+1}^T\right) = R \tag{4}$$

The matrices A, b, C, and Γ are known. The respective Gaussian zero mean process noise and measurement noise covariance matrices, Q and R, are also known. The open-loop gain K is not known.

Denote by $\hat{x}_k$ and $\hat{K}_k$ the respective estimates of the state x_k and the loop gain K at time k, given the measurements record $z_1, \ldots, z_k$,

Received 8 November 2001; revision received 10 April 2002; accepted for publication 10 June 2002.

*Professor, Department of Electrical Engineering. Associate Fellow AIAA.
†Ph.D. Student, Department of Electrical Engineering.

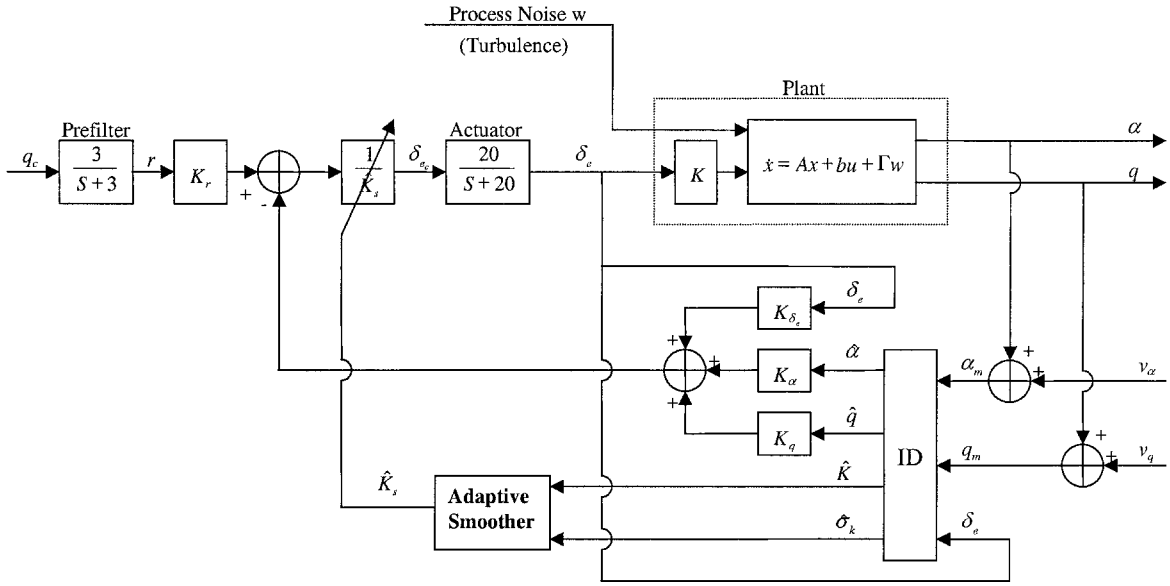

Fig. 1 Adaptive and reconfigurable flight control system.

the input sequence $u_0, \ldots, u_{k-1}$, and the prior information on x_0 and K. The covariance of the estimation error of the

$$\begin{pmatrix} x_k \\ K \end{pmatrix}$$

vector is denoted by the partitioned matrix

$$P_k = \begin{pmatrix} P_{k_{xx}} & p_{k_{xK}} \\ p_{k_{xK}}^T & p_{k_{KK}} \end{pmatrix}$$

Initially, set

$$\hat{x}_0 \equiv \bar{x}_0, \qquad \hat{K}_0 \equiv \stackrel{\Delta}{=} K_0, \qquad P_{0_{xx}} \equiv \stackrel{\Delta}{=} P_{0_x}$$

$$p_{0_{KK}} \equiv \stackrel{\Delta}{=} P_{0_K}, \qquad p_{0_{xK}} \equiv \stackrel{\Delta}{=} 0 \tag{5}$$

Then, for $k = 0, 1, \ldots, N-1$, the state and gain estimates are updated as

$$\hat{x}_{k+1} = A\hat{x}_k + \hat{K}_k b u_k + K_x(z_{k+1} - CA\hat{x}_k - \hat{K}_k C b u_k) \tag{6}$$

$$\hat{K}_{k+1} = \hat{K}_k + K_K(z_{k+1} - CA\hat{x}_k - \hat{K}_k C b u_k) \tag{7}$$

where the Kalman gains

$$K_x = \left\{ AP_{k_{xx}}A^TC^T + u_k\left[Ap_{k_{xK}}(Cb)^T + b\left(CAp_{k_{xK}}\right)^T\right] + u_k^2 p_{k_{KK}} b(Cb)^T + \Gamma Q\Gamma^T C^T \right\} \times \left\{ CAP_{k_{xx}}A^TC^T + u_k\left[CAp_{k_{xK}}(Cb)^T + (Cb)\left(CAp_{k_{xK}}\right)^T\right] + u_k^2 p_{k_{KK}}(Cb)(Cb)^T + C\Gamma Q\Gamma^T C^T + R \right\}^{-1} \tag{8}$$

$$K_K = \left[\left(CAp_{k_{xK}}\right)^T + u_k p_{k_{KK}}(Cb)^T \right] \times \left\{ CAP_{k_{xx}}A^TC^T + u_k\left[CAp_{k_{xK}}(Cb)^T + (Cb)\left(CAp_{k_{xK}}\right)^T\right] + u_k^2 p_{k_{KK}}(Cb)(Cb)^T + C\Gamma Q\Gamma^T C^T + R \right\}^{-1} \tag{9}$$

Furthermore, the estimation error covariances are

$$P_{k+1_{xx}} = \left\{ \left[AP_{k_{xx}}A^T + u_k\left(Ap_{k_{xK}}b^T + bp_{k_{xK}}^T A^T\right)\right] + u_k^2 p_{k_{KK}} bb^T + \Gamma Q\Gamma^T \right]^{-1} + C^T R^{-1} C \Bigg\}^{-1} \tag{10}$$

$$p_{k+1_{KK}} = p_{k_{KK}} - \left[\left(CAp_{k_{xK}}\right)^T + u_k p_{k_{KK}}(Cb)^T \right] \times \left\{ CAP_{k_{xx}}A^TC^T + u_k\left[CAp_{k_{xK}}(Cb)^T + (Cb)\left(CAp_{k_{xK}}\right)^T\right] + u_k^2 p_{k_{KK}}(Cb)(Cb)^T + C\Gamma Q\Gamma^T C^T + R \right\}^{-1} \times \left[\left(CAp_{k_{xK}}\right) + u_k p_{k_{KK}}(Cb) \right] \tag{11}$$

$$p_{k+1_{xK}} = Ap_{k_{xK}} + u_k p_{k_{KK}} b - \left\{ AP_{k_{xx}}A^TC^T + u_k\left[Ap_{k_{xK}}(Cb)^T + b(CAp_{k_{xK}})^T\right] + u_k^2 p_{k_{KK}} b(Cb)^T + \Gamma Q\Gamma^T C^T \right\} \times \left\{ CAP_{k_{xx}}A^TC^T + u_k\left[CAp_{k_{xK}}(Cb)^T + (Cb)\left(CAp_{k_{xK}}\right)^T\right] + u_k^2 p_{k_{KK}}(Cb)(Cb)^T + C\Gamma Q\Gamma^T C^T + R \right\}^{-1} \times \left[\left(CAp_{k_{xK}}\right) + u_k p_{k_{KK}}(Cb) \right] \tag{12}$$

The proof of the Theorem is relegated to the Appendix, where it is also shown how the classical Kalman filtering algorithm is recovered in the special case where the loop gain parameter is known.

III. Adaptive Parameter Smoothing

In Ref. 6, a fixed low-pass filter that exclusively operates on the parameter estimate provided by the system identification algorithm was used to smooth the parameter estimate. Note, however, that the fixed low-pass filter does not use the available predicted parameter estimation error variance, which is indicative of the level of excitation in the identification experiment and is reliably provided by the system identification algorithm. Using the predicted estimation error variance information that is provided by our rigorous system identification algorithm, one can selectively employ smoothing. Indeed, when the parameter estimation error variance is small, we can employ assumed certainty equivalence, because then we know that the parameter estimate must be close to the true parameter value, provided that the computed error variance is reliable. Then, there is no need to filter the parameter estimate, and therefore, the lag caused by passing the parameter estimate through a low-pass filter is now removed. If, however, the parameter estimation error variance is large and we are not confident using the system identification (provided parameter estimate in the compensator synthesis), it is then advantageous to rely on filtering. This is tantamount to postulating that the parameter does not change much during the short time interval under consideration. Therefore, in the online compensator synthesis, we partially rely on the old parameter estimate. In this case, one introduces some lag.

Hence, we now make the filter dynamics dependent on the parameter estimation error variance provided by the upstream system identification module, and in doing so, we adaptively filter the loop gain estimate. These insights into the estimation situation at hand suggest the following strategy: Set the weight of the current parameter estimate provided by the system identification algorithm, $1-\lambda_k$, as follows:

$$\log_{10}(1-\lambda_k) = 1/10^{(\mathrm{SNR}_k - \mathrm{SNR}_{k-w_l})}$$

where the SNR in the system identification experiment at time k is now defined as

$$\mathrm{SNR}_k = 20\log_{10}\left(K/\sigma_{K_k}\right)$$

and w_l is the moving window length used in the system identification algorithm and $\sigma_{K_k} = \sqrt{p_{kKK}}$. Thus, a decrease in the SNR caused by a sudden increase in the predicted parameter estimation error σ_K as one moves from estimation window $k-w_l$ to estimation window k has the effect of decreasing the reliance on the most recent loop gain estimate $\hat{K}_k$. When the excitation is low, one would like to shut down the system identification algorithm and freeze the parameter estimate at its previous value.

Hence, the adaptive filter for the parameter estimate is

$$\hat{K}_{k_{\mathrm{smoothed}}} = \lambda_k \times \hat{K}_{k-1_{\mathrm{smoothed}}} + (1-\lambda_k)\times \hat{K}_k \tag{13}$$

where the weight λ_k, $0<\lambda_k<1$, is adjusted according to

$$\lambda_k = 1 - 10^{-\left(\sigma_{K_k}/\sigma_{K_{k-w_l}}\right)^{10}} \tag{14}$$

and where σ_{K_k} is the predicted parameter K estimation error variance provided by the system identification module at time instant k.

The adaptive parameter estimate filter [Eqs. (13) and (14)] automatically smoothes the parameter estimate and precludes bursting.

IV. Aircraft Model and Fixed PI Controller

A. Aircraft Model

In this paper, an F-16 class aircraft flying at Mach 0.9 at 20,000 ft is considered. The short-period pitch dynamics approximation[9] is used. The pitch dynamics are unstable, and hence, the aircraft relies on feedback control for stabilization. The relevant states are α and q, the aircraft angle of attack and pitch rate, respectively, and the control variable is the elevator deflection δ_e. Thus, the plant truth model used in the system identification algorithm is

$$\dot{\alpha} = Z_\alpha\alpha + Z_q q + KZ_{\delta_e}\delta_e, \qquad \dot{q} = M_\alpha\alpha + M_q q + KM_{\delta_e}\delta_e$$

The Z stability and control derivatives are

$$Z_\alpha = -1.3433, \qquad Z_q = 0.9946, \qquad Z_{\delta_e} = -0.1525$$

and the M stability and control derivatives are

$$M_\alpha = 3.5, \qquad M_q = -1.0521, \qquad M_{\delta_e} = -24.3282$$

Hence, in (continuous-time) state-space form, the bare aircraft (plant) dynamics are

$$\dot{x} = Ax + bu = \begin{pmatrix} -1.3433 & 0.9946 \\ 3.5 & -1.0521 \end{pmatrix} x + \begin{pmatrix} -0.1525 \\ -24.3282 \end{pmatrix} u \tag{15}$$

where the state

$$x = \begin{pmatrix} \alpha \\ q \end{pmatrix}$$

and the control variable u is the elevator deflection δ_e in degrees.

The preceding second-order plant model is the truth model used in the system identification algorithm.

In the linear tracking controller, the reference signal r is summed with the states α and q feedback.

The controller-generated command to the elevator δ_{e_c} is applied to a first-order actuator model

$$\delta_e(s)/\delta_{ec}(s) = 20/(s+20) \tag{16}$$

with a bandwidth of 20 rad/s. The actuator output δ_e is the input to the plant. A first-order actuator model suffices in the low-frequency bandwidth of the pitch dynamics. A more elaborate fourth-order actuator model is

$$\frac{\delta_e(s)}{\delta_{ec}(s)} = \frac{(20.2)(5097.96)(144.8)}{(s+20.2)(s^2+1008s+5097.96)(s+144.8)}$$

however, the first-order actuator model captures the lag characteristics of the actuator in the bandwidth of interest.

Augmenting the dynamics and control matrices with the first-order actuator dynamics yields the third-order augmented plant

$$\dot{x} = Ax + bu = \begin{pmatrix} Z_\alpha & Z_q & Z_{\delta_e} \\ M_\alpha & M_q & M_{\delta_e} \\ 0 & 0 & -1/\tau \end{pmatrix} x + \begin{pmatrix} 0 \\ 0 \\ 1/\tau \end{pmatrix} \delta_{e_c}$$

where $\tau = \frac{1}{20} = 0.05$ s. Now the states are

$$x = (\alpha \quad q \quad \delta_e)^T$$

and the control variable is δ_{e_c}.

The preceding third-order plant model is the truth model used for tracking controller design.

B. Fixed PI Controller

The design of the model-based PI tracking controller follows the development in Ref. 10. Designing a PI controller in state space for good tracking performance requires the system dynamics to be further augmented. Now

$$\dot{z} = r - q$$

$$\dot{x} = \begin{pmatrix} Z_\alpha & Z_q & Z_{\delta_e} & 0 \\ M_\alpha & M_q & M_{\delta_e} & 0 \\ 0 & 0 & -1/\tau & 0 \\ 0 & -1 & 0 & 0 \end{pmatrix} x + \begin{pmatrix} 0 \\ 0 \\ 0 \\ 1 \end{pmatrix} r + \begin{pmatrix} 0 \\ 0 \\ 1/\tau \\ 0 \end{pmatrix} \delta_{e_c}$$

where the states are now

$$x = (\alpha \quad q \quad \delta_e \quad z)^T$$

and, as before, r is the reference signal. The charge on the integrator is z. Now the PI control law is

$$\delta_{e_c} = r - K_\alpha\alpha - K_q q - K_{\delta_e}\delta_e + K_z z \tag{17}$$

The PI gains needed to obtain good tracking performance are

$$K_\alpha = 0.283, \qquad K_q = 0.876, \qquad K_{\delta_e} = -0.4, \qquad K_z = 0.01$$

The new closed-loop system matrices A_{cl} and B_{cl} are

$$A_{\mathrm{cl}} = A + b\begin{pmatrix} -K_\alpha & -K_q & -K_{\delta_e} & K_z \end{pmatrix} = \begin{pmatrix} Z_\alpha & Z_q & Z_{\delta_e} & 0 \\ M_\alpha & M_q & M_{\delta_e} & 0 \\ -K_\alpha/\tau & -K_q/\tau & -(1+K_{\delta_e})/\tau & K_z/\tau \\ 0 & -1 & 0 & 0 \end{pmatrix}$$

$$B_{\mathrm{cl}} = \begin{pmatrix} 0 & 0 & 1/\tau & 1 \end{pmatrix}^T$$

B_{cl} operates on the exogeneous (reference) signal r.

The F-16 class plant is open-loop unstable. This is a normal characteristic of advanced fighter aircraft. Using full state feedback, the

flight control system is stabilized. Tracking is achieved using the fixed PI controller specified in Eq. (17).

V. Simulation

A. Estimation Performance

The estimation performance guaranteed by the novel system identification algorithm stated in the theorem is experimentally validated, and the results of the open-loop gain identification experiments are presented.

A moving window (or, equivalently, finite memory data window) is used because, in the case of a failure, when a jump in the value of the open-loop gain K occurs the latter is identified faster than in the case where an expanding horizon window system identification algorithm is used. At time k, the moving window consists of the samples taken at time $k - w_l + 1, \ldots, k$; the expanding window is of length k and consists of the samples taken at time $1, \ldots, k$. When the recursive system identification algorithm (the theorem in Sec. II) is used inside a 0.3-s window (of 30 samples), estimates of the parameters of interest are calculated. The window is then shifted one sample time, and the estimation process is repeated. This yields the first parameter estimate at 0.3 s into the flight. Prior information with negative α and q states and an initial guess of $K = 0.8$ are intentionally used to test the moving window estimation algorithm's response to a poor initial guess. For all of the windows, the same prior information of $\alpha = -1.4414$ deg, $q = -2.4314$ deg/s,

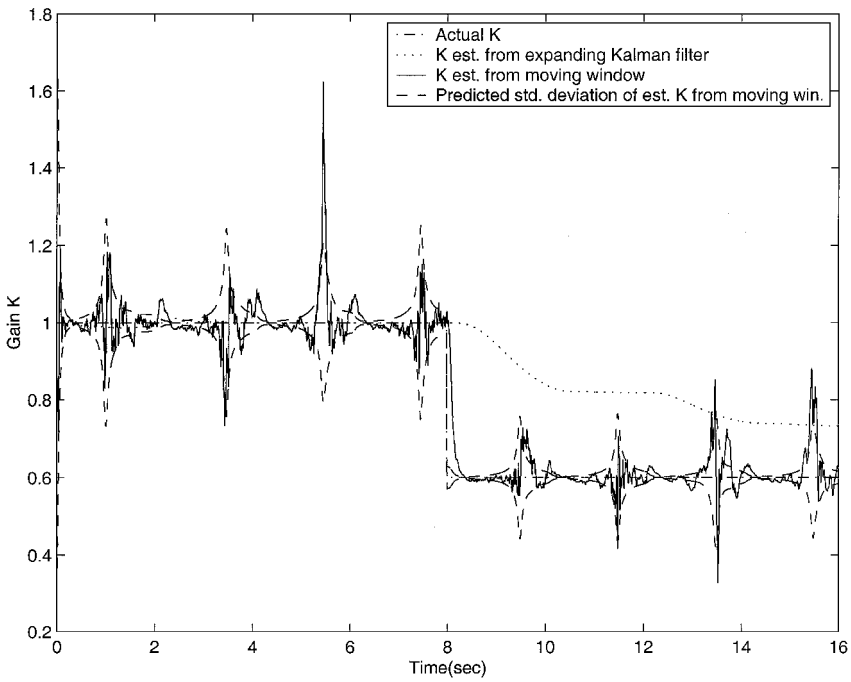

Fig. 2 Comparison of expanding horizon and moving window estimation with fixed PI tracking controller: $\sigma_\alpha = 0.03$ deg, $\sigma_q = 0.1108$ deg/s, and $K_1 = 0.6$ at 8 s.

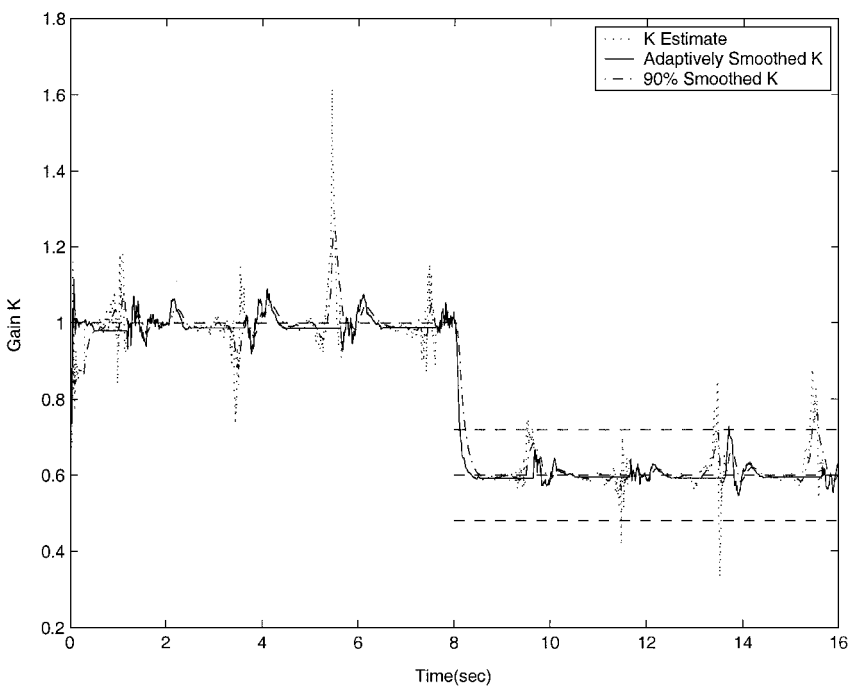

Fig. 3 Loop gain estimate $\hat{K}$ and smoothed $\hat{K}_s$ when moving window system identification, fixed weights smoother, and adaptive smoother are used: $\sigma_\alpha = 0.03$ deg, $\sigma_q = 0.1108$ deg/s, and $K_1 = 0.6$ at 8 s; unsmoothed K_e vs smoothed K_e.

and $K = 0.8$ is used. The initial states α and q variances are 0.1 deg^2 and 1 (deg/s)^2, respectively, and the relatively high variance of the parameter K initial guess is 0.4.

Setting the postfailure open-loop gain at $K_1 = 0.6$, we compare in Fig. 2 the open-loop gain $\hat{K}$ estimation performance of the moving window system identification algorithm and the expanding window system identification algorithm. The fixed PI tracking controller, and no parameter estimate filter, is used. One can see that the moving window is faster to settle on an estimate, whereas the expanding horizon system identification algorithm takes more time to reach its final estimate value. Obviously, the estimate provided by the expanding window Kalman filter is smoother than the estimate provided by the relatively short sliding window. At the same time, in Fig. 2, the negative effect on estimation performance of a very short window ($\ll 0.3$ s) is also evident near $t = 0$.

B. Adaptive Parameter Estimate Smoother

A fixed-weights smoother acts similarly to a longer estimation window and will reduce the fluctuations in $\hat{K}$, but it will uniformly increase the identification delay, and, consequently, response time of the identification algorithm, as shown in Ref. 7. Thus, in Fig. 3, we see that the adaptive smoother [Eq. (13)] not only yields the fastest identification time, but also is more effective than a fixed-weights smoother; the dotted lines designate K_1 error bounds of $\pm 20\%$.

C. Tracking Performance

In the simulation experiments, at time $t = 8$ s into the flight, the open-loop gain K is reduced to $K_1 = 0.1$. The fixed linear PI tracking controller design in Sec. IV is exercised first, for example, see Fig. 4. Next, the tracking performance of our adaptive and reconfigurable control system is evaluated. In Fig. 5, a two-module adaptive and

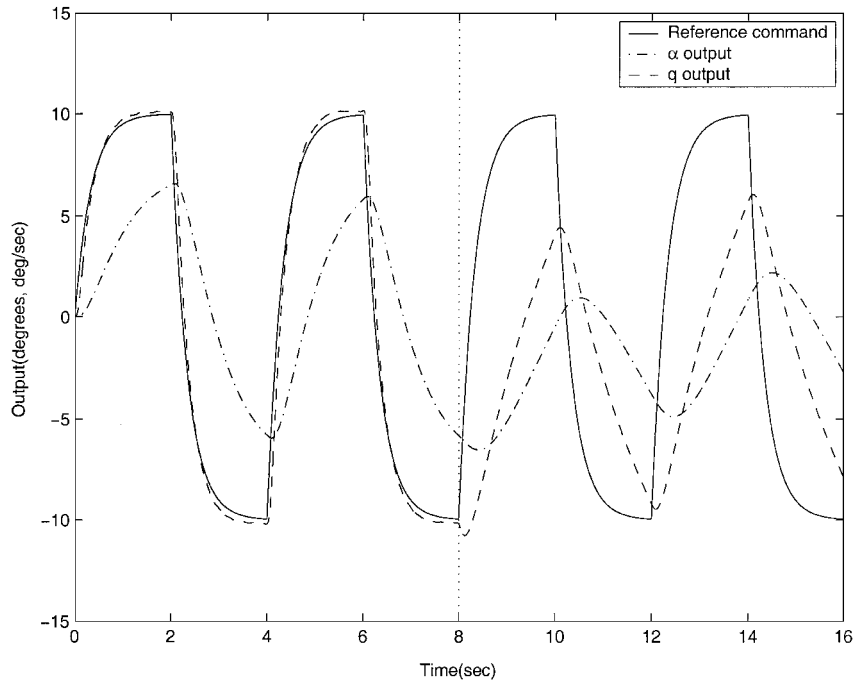

Fig. 4 With fixed PI controller used, q and α responses: σ_α = 0.03 deg, σ_q = 0.1108 deg/s, and K_1 = 0.1; short-period outputs and failure K = 0.1 at 8 s.

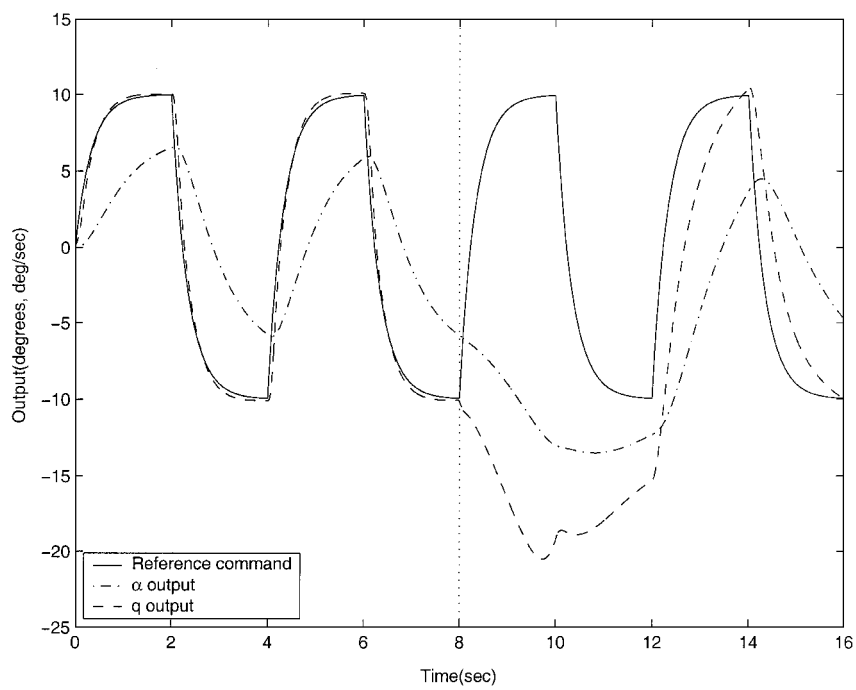

Fig. 5 With expanding window system identification algorithm and reconfigurable control used, q and α responses: σ_α = 0.03 deg, σ_q = 0.1108 deg/s, and K_1 = 0.1; short-period outputs, failure K = 0.1 at 8 s.

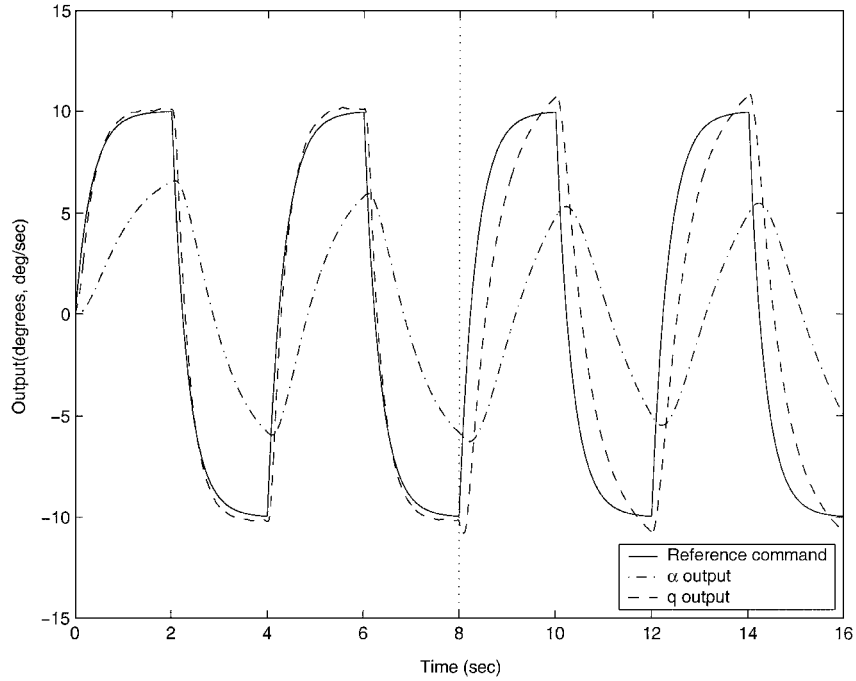

Fig. 6 With moving window system identification algorithm and adaptive smoother used; q and α response: $\sigma_\alpha = 0.03$ deg, $\sigma_q = 0.1108$ deg/s, and $K_1 = 0.1$; short-period outputs, failure $K = 0.1$ at 8 s.

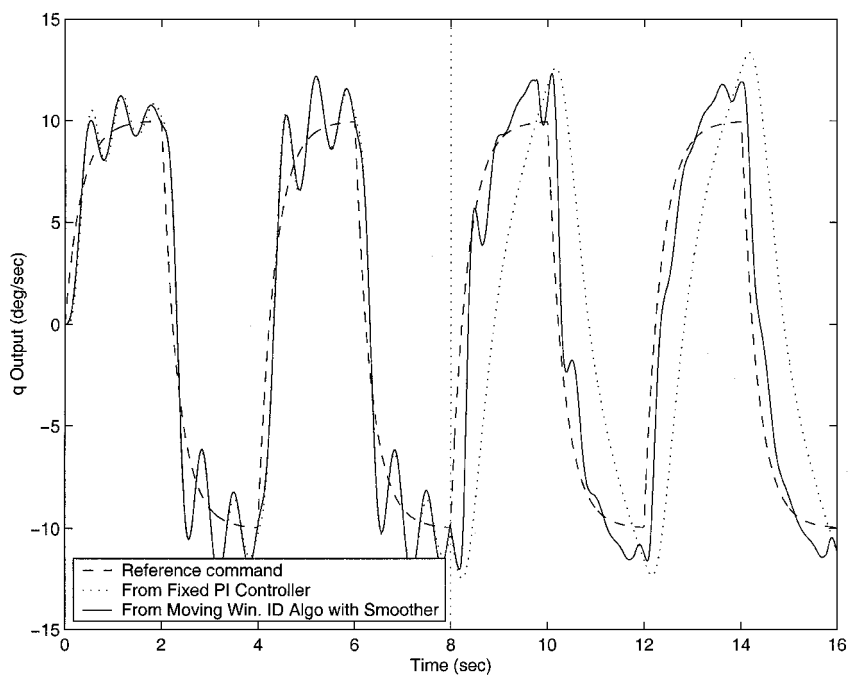

Fig. 7 Comparison of the tracking performance of the fixed PI controller and the adaptive and reconfigurable controller; phugoid dynamics, fourth-order actuator model, and parametric modeling error ($M_\alpha = 5$ after failure) are included: q output, $K_{\delta_e} = -0.4$, $\sigma_\alpha = 0.03$ deg, $\sigma_q = 0.1108$ deg/s, and $K_1 = 0.2$; failure $K = 0.2$ at 8 s $K_{\delta_e} = -0.4$.

reconfigurable controller consisting of an expanding window system identification module and a reconfigurable PI controller is used. In Fig. 6, the three-module controller with a moving window system identification module is used.

When the open-loop gain K decreases to $K_1 = 0.1$, postfailure tracking performance of the fixed PI controller deteriorates significantly and is not acceptable. When a conventional, two-module, adaptive and reconfigurable controller is implemented immediately after the point of failure at $t = t_f = 8$ s, a considerable error between the aircraft's pitch rate and the commanded pitch rate develops. This is mainly due to the estimation lag in the expanding window system identification module. However, the tracking performance improves as time passes, and the expanding window system identification algorithm settles on a good parameter estimate; consequently, the pitch rate then tracks the commanded pitch rate. The tracking performance of the complete, three-module, adaptive, and reconfigurable controller, using the moving window system identification algorithm, is shown in Fig. 6. After the failure, only a small tracking error occurs between the commanded pitch rate and the pitch rate output. However, the tracking performance is much better than that of the fixed PI tracking controller and the earlier discussed two-module adaptive tracking controller using an expanding window-based system identification algorithm.

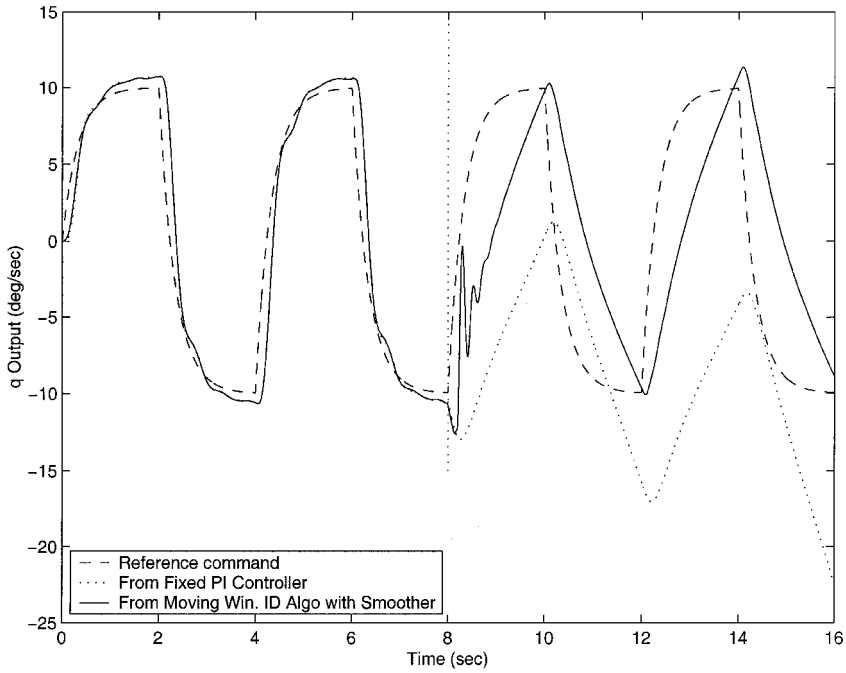

Fig. 8 Comparison of the tracking performance of the fixed PI controller and the adaptive and reconfigurable controller; phugoid dynamics, fourth-order actuator model, and parametric modeling error ($M_\alpha = 5$ after failure) are included: q output, $K_{\delta_e} = -1.5$, $\sigma_\alpha = 0.03$ deg, $\sigma_q = 0.1108$ deg/s, and $K_1 = 0.2$; failure $K = 0.2$ at 8 s $K_{\delta_e} = -1.5$.

D. Unmodeled Dynamics Effects on Identification and Tracking Performance

We now include in our realistic simulation the phugoid dynamics, use the fourth-order actuator model, and allow for a postfailure parameter modeling error ($M_\alpha = 5$). We investigate their cumulative effect on identification and tracking performance. The moving window parameter identification algorithm and the adaptive smoother are used.

Figure 7 shows the tracking performance of the fixed PI controller and the three-module adaptive and reconfigurable controller (moving-window system identification algorithm with adaptive smoother). We also set the control gain to the original $K_{\delta_e} = -0.4$, and the control surface failure index is $K_1 = 0.2$. After the failure, the adaptive and reconfigurable controller outperforms the fixed PI controller, in particular, in the severe failure case of $K_1 = 0.2$, where the fixed PI controller's tracking performance is poor.

When we change the control gain K_{δ_e} to -1.5, the results are shown in Fig. 8. The adaptive and reconfigurable controller outperforms the fixed PI controller in all failure cases. In the case of a severe failure ($K_1 = 0.2$), the adaptive and reconfigurable controller shows some lag in tracking, but the fixed PI controller causes a departure.

VI. Conclusions

A novel three-module fault tolerant flight control system consisting of 1) a system identification module, 2) an adaptive parameter estimate smoother, and 3) a robust PI compensator for tracking control is developed.

System identification lies at the heart of indirect adaptive and reconfigurable control. The novel and rigorous system identification algorithm provides an unbiased loop gain parameter estimate and a reliable predicted parameter estimation error variance. This is confirmed by the carefully designed simulation experiments: The system identification algorithm performs well using small samples and in the presence of measurement noise, weak excitation, unmodeled dynamics, and parametric uncertainty. Online operation is achieved, and no human intervention is required.

High levels of measurement noise, small sample size, and poor excitation increase the parameter estimation error variance, and this causes the parameter estimate to fluctuate as we move from window to window. The role of the parameter estimate smoother is 1) to reduce low excitation-induced fluctuations in the parameter estimate before using the latter in the downstream online controller synthesis algorithm and 2) to address the ill effects of modeling error and, in particular, parametric modeling error on the performance of the system identification algorithm. The innovative adaptive parameter estimate smoother uses all of the available information on the plant parameter provided by the upstream online system identification module. Hence, the lag and the error in the plant parameter estimate calculated by the smoother and sent to the compensator is minimized.

A carefully designed model-based robust PI tracking controller using full state feedback was used. This is the baseline controller against which the performance of the adaptive and reconfigurable controller is evaluated. In the adaptive and reconfigurable controller, the reciprocal of the estimated loop gain derived from the system identification algorithm and processed by the smoothing module is used online to adjust the compensator, to account for the effector failure, and, thus, to recover performance.

The three-module adaptive and reconfigurable controller uses a sampling rate of 100 Hz, a sliding data window of 0.3 s, a formula for setting the weights of the adaptive parameter smoother, and a model-based PI controller. Although the design of each of the three modules of the controller is solidly rooted in theory, the adaptive and reconfigurable flight control system is a nonlinear stochastic control system with partial observations and there is heavy reliance on the carefully designed simulation experiments. The simulation experiments validate the performance of the adaptive and reconfigurable controller: The tracking performance of the complete adaptive and reconfigurable control system is shown to be superior to the tracking performance of the robust, but fixed, PI tracking controller, in particular, in the case of a severe failure (80% control surface loss). The simulation experiments demonstrate that with the fixed PI controller, in the case of a severe failure, a departure is on hand, whereas the adaptive and reconfigurable controller yields acceptable tracking performance.

The adaptive and reconfigurable controller design methodology developed in this paper is illustrated in a flight control context. However, this development is applicable to a broad range of control problems.

Appendix: Proof of Theorem

We shall require the complete matrix inversion lemma (MIL).

Lemma (MIL): Assume the relevant matrices are compatible and invertible. Then

$$\left(A_1 - A_2 A_4^{-1} A_3\right)^{-1} = A_1^{-1} + A_1^{-1} A_2 \left(A_4 - A_3 A_1^{-1} A_2\right)^{-1} A_3 A_1^{-1} \tag{A1}$$

□

Proof of Theorem: Because the unknown loop gain is a constant, we augment the dynamics as follows:

$$K_{k+1} = K_k \tag{A2}$$

Hence, the augmented state dynamics evolve in $\Re^{n+1}$ and are

$$\begin{pmatrix} x_{k+1} \\ K_{k+1} \end{pmatrix} = \begin{pmatrix} A & u_k b \\ 0 & 1 \end{pmatrix} \begin{pmatrix} x_k \\ K_k \end{pmatrix} + \begin{pmatrix} \Gamma \\ 0 \end{pmatrix} w_k \tag{A3}$$

and the measurement equation is

$$z_{k+1} = \begin{pmatrix} C & \vdots & 0 \end{pmatrix} \begin{pmatrix} x_{k+1} \\ K_{k+1} \end{pmatrix} + v_{k+1} \tag{A4}$$

Here, w_k and v_{k+1} represent the process noise and measurement noise, respectively. The covariances of these noises are represented by Q and R in the stochastic model.

The prior information at time instant k is

$$\begin{pmatrix} x_k \\ K_k \end{pmatrix} \in N\left[\begin{pmatrix} \hat{x}_k \\ \hat{K}_k \end{pmatrix}, \quad P_k \right] \tag{A5}$$

where

$$P_k = \begin{pmatrix} P_{k_{xx}} & p_{k_{xK}} \\ p_{k_{xK}}^T & p_{k_{KK}} \end{pmatrix} \tag{A6}$$

is the estimation error covariance matrix. The elements of P_k are

$$P_{k_{xx}} \in \Re^{n \times n}, \qquad p_{k_{xK}} \in \Re^n, \qquad p_{k_{KK}} \in \Re^1 \tag{A7}$$

Hence, before the z_{k+1} measurement is recorded, the augmented state

$$\begin{pmatrix} x_{k+1} \\ K_{k+1} \end{pmatrix} \in N\left(\begin{pmatrix} A & u_k b \\ 0 & 1 \end{pmatrix} \begin{pmatrix} \hat{x}_k \\ \hat{K}_k \end{pmatrix} \right.$$

$$\left. \begin{pmatrix} A & u_k b \\ 0 & 1 \end{pmatrix} P_k \begin{pmatrix} A^T & 0 \\ u_k b^T & 1 \end{pmatrix} + \begin{pmatrix} \Gamma Q \Gamma^T & 0 \\ 0 & 0 \end{pmatrix} \right)$$

$$= N\left(\begin{pmatrix} A\hat{x}_k + \hat{K}_k b u_k \\ \hat{K}_k \end{pmatrix} \right.$$

$$\left. \begin{pmatrix} AP_{k_{xx}}A^T + u_k\left(Ap_{k_{xK}} b^T + \right. & \vdots & \\ \left. bp_{k_{xK}}^T A^T\right) + u_k^2 p_{k_{KK}} bb^T + \Gamma Q \Gamma^T & \vdots & Ap_{k_{xK}} + u_k p_{k_{KK}} b \\ \cdots\cdots\cdots\cdots\cdots\cdots & \vdots & \cdots\cdots\cdots \\ p_{k_{xK}}^T A^T + u_k p_{k_{KK}} b^T & \vdots & p_{k_{KK}} \end{pmatrix} \right)$$

Next, apply the Bayesian estimation formula and obtain

$$\hat{x}_k^+ = \hat{x}_k^- + K(z - H\hat{x}_k) \tag{A8}$$

$$\begin{pmatrix} \hat{x}_{k+1} \\ \hat{K}_{k+1} \end{pmatrix} = \begin{pmatrix} A\hat{x}_k + \hat{K}_k b u_k \\ \hat{K}_k \end{pmatrix} + K\left(z_{k+1} \right.$$

$$\left. - \begin{pmatrix} C & \vdots & 0 \end{pmatrix} \begin{pmatrix} A\hat{x}_k + \hat{K}_k b u_k \\ \hat{K}_k \end{pmatrix} \right) = \begin{pmatrix} A\hat{x}_k + \hat{K}_k b u_k \\ \hat{K}_k \end{pmatrix}$$

$$+ K(z_{k+1} - CA\hat{x}_k - u_k \hat{K}_k Cb) \tag{A9}$$

where the Kalman gain

$$K = \begin{pmatrix} AP_{k_{xx}}A^T + u_k\left(Ap_{k_{xK}} b^T + \right. & \vdots \\ \left. bp_{k_{xK}}^T A^T\right) + u_k^2 p_{k_{KK}} bb^T + \Gamma Q \Gamma^T & \vdots \\ \cdots\cdots\cdots\cdots\cdots\cdots & \vdots \\ p_{k_{xK}}^T A^T + u_k p_{k_{KK}} b^T & \vdots \end{pmatrix}$$

$$\begin{pmatrix} \vdots & Ap_{k_{xK}} + u_k p_{k_{KK}} b \\ \vdots & \cdots\cdots\cdots \\ \vdots & p_{k_{KK}} \end{pmatrix} \times \begin{pmatrix} C^T \\ 0 \end{pmatrix} \times \left\{ CAP_{k_{xx}} A^T C^T \right.$$

$$+ u_k\left[CAp_{k_{xK}} (Cb)^T + (Cb)(CAp_{k_{xK}})^T \right]$$

$$\left. + u_k^2 p_{k_{KK}} (Cb)(Cb)^T + C\Gamma Q \Gamma^T C^T + R \right\}^{-1}$$

$$= \begin{pmatrix} AP_{k_{xx}}A^T C^T \\ +u_k\left[Ap_{k_{xK}} (Cb)^T + b\left(CAp_{k_{xK}}\right)^T \right] \\ +u_k^2 p_{k_{KK}} b(Cb)^T + \Gamma Q \Gamma^T C^T \\ \cdots\cdots\cdots\cdots\cdots\cdots\cdots\cdots \\ \left(CAp_{k_{xK}}\right)^T + u_k p_{k_{KK}} (Cb)^T \end{pmatrix} \times \left\{ CAP_{k_{xx}} A^T C^T \right.$$

$$+ u_k\left[CAp_{k_{xK}} (Cb)^T + (Cb)\left(CAp_{k_{xK}}\right)^T \right]$$

$$\left. + u_k^2 p_{k_{KK}} (Cb)(Cb)^T + C\Gamma Q \Gamma^T C^T + R \right\}^{-1} \tag{A10}$$

Finally,

$$P_{k+1_{(x,K)}} = P_{k_{(x,K)}} - K\begin{pmatrix} C & \vdots & 0 \end{pmatrix} P_{k_{(x,K)}} \tag{A11}$$

Hence, we calculate

$$P_{k+1_{(x,K)}}$$

$$= \begin{pmatrix} AP_{k_{xx}}A^T + u_k\left(Ap_{k_{xK}} b^T + \right. & \vdots & \\ \left. bp_{k_{xK}}^T A^T\right) + u_k^2 p_{k_{KK}} bb^T + \Gamma Q \Gamma^T & \vdots & Ap_{k_{xK}} + u_k p_{k_{KK}} b \\ \cdots\cdots\cdots\cdots\cdots\cdots & \vdots & \cdots\cdots\cdots \\ p_{k_{xK}}^T A^T + u_k p_{k_{KK}} b^T & \vdots & p_{k_{KK}} \end{pmatrix}$$

$$- \begin{pmatrix} \left\{ AP_{k_{xx}}A^T C^T \right. & \vdots \\ +u_k\left[Ap_{k_{xK}} (Cb)^T + b\left(CAp_{k_{xK}}\right)^T \right] & \vdots \\ \left. +u_k^2 p_{k_{KK}} b(Cb)^T + \Gamma Q \Gamma^T C^T \right\} & \vdots \\ \times\left\{ CAP_{k_{xx}} A^T C^T \right. & \vdots \\ +u_k\left[CAp_{k_{xK}} (Cb)^T + (Cb)(CAp_{k_{xK}})^T \right] & \vdots \\ \left. + u_k^2 p_{k_{KK}} (Cb)(Cb)^T + C\Gamma Q \Gamma^T C^T + R \right\}^{-1} & \vdots \\ \times\left[CAp_{k_{xx}} A^T + u_k\left(CAp_{k_{xK}} b^T + CbAp_{k_{xK}}^T A^T\right) \right. & \vdots \\ \left. + u_k^2 p_{k_{KK}} Cbb^T + C\Gamma Q \Gamma^T \right] & \vdots \\ \cdots\cdots\cdots\cdots\cdots\cdots\cdots\cdots\cdots\cdots & \vdots \\ \left[\left(CAp_{k_{xK}}\right)^T + u_k p_{k_{KK}} (Cb)^T \right] & \\ \times\left\{ CAP_{k_{xx}} A^T C^T \right. & \vdots \\ +u_k\left[CAp_{k_{xK}} (Cb)^T + (Cb)\left(CAp_{k_{xK}}\right)^T \right] & \vdots \\ \left. + u_k^2 p_{k_{KK}} (Cb)(Cb)^T + C\Gamma Q \Gamma^T C^T + R \right\}^{-1} & \vdots \\ \times\left[CAP_{k_{xx}} A^T + u_k\left(CAp_{k_{xK}} b^T + CbAp_{k_{xK}}^T A^T\right) \right. & \vdots \\ \left. + u_k^2 p_{k_{KK}} Cbb^T + C\Gamma Q \Gamma^T \right] & \end{pmatrix}$$

$$
\begin{array}{l}
\left\{AP_{k_{xx}}A^TC^T + u_k\left[Ap_{k_{xK}}(Cb)^T + b\left(CAp_{k_{xK}}\right)^T\right]\right. \\
\left. + u_k^2 p_{k_{KK}} b(Cb)^T + \Gamma Q \Gamma^T C^T\right\} \\
\times\left\{CAP_{k_{xx}}A^TC^T + u_k\left[CAp_{k_{xK}}(Cb)^T + (Cb)\left(CAp_{k_{xK}}\right)^T\right]\right. \\
\left. + u_k^2 p_{k_{KK}}(Cb)(Cb)^T + C\Gamma Q\Gamma^T C^T + R\right\}^{-1} \\
\times\left(CAp_{k_{xK}} + u_k p_{k_{KK}} Cb\right) \\
\hline
\left[\left(CAp_{k_{xK}}\right)^T + u_k p_{k_{KK}}(Cb)^T\right] \\
\times\left\{CAP_{k_{xx}}A^TC^T + u_k\left[CAp_{k_{xK}}(Cb)^T + (Cb)\left(CAp_{k_{xK}}\right)^T\right]\right. \\
\left. + u_k^2 p_{k_{KK}}(Cb)(Cb)^T + C\Gamma Q\Gamma^T C^T + R\right\}^{-1} \\
\times\left(CAp_{k_{xK}} + u_k p_{k_{KK}} Cb\right)
\end{array}
\Bigg) \tag{A12}
$$

Thus,

$$
\begin{aligned}
P_{k+1_{xx}} = {} & \left[AP_{k_{xx}}A^T + u_k\left(Ap_{k_{xK}}b^T + bp_{k_{xK}}^T A^T\right)\right. \\
& \left. + u_k^2 p_{k_{KK}} bb^T + \Gamma Q\Gamma^T\right] \times \left\{\left[AP_{k_{xx}}A^T\right.\right. \\
& \left. + u_k\left(Ap_{k_{xK}}b^T + bp_{k_{xK}}^T A^T\right) + u_k^2 p_{k_{KK}} bb^T + \Gamma Q\Gamma^T\right]^{-1} \\
& - C^T\left\{CAP_{k_{xx}}A^TC^T + u_k\left[CAp_{k_{xK}}(Cb)^T + (Cb)\left(CAp_{k_{xK}}\right)^T\right]\right. \\
& \left.\left. + u_k^2 p_{k_{KK}}(Cb)(Cb)^T + C\Gamma Q\Gamma^T C^T + R\right\}^{-1} C\right\} \times \left[AP_{k_{xx}}A^T\right. \\
& \left. + u_k\left(Ap_{k_{xK}}b^T + bp_{k_{xK}}^T A^T\right) + u_k^2 p_{k_{KK}} bb^T + \Gamma Q\Gamma^T\right]
\end{aligned} \tag{A13}
$$

Next, apply the MIL to the expression in the outer braces from Eq. (A14), namely,

$$
\begin{aligned}
& \left\{\left[AP_{k_{xx}}A^T + u_k\left(Ap_{k_{xK}}b^T + bp_{k_{xK}}^T A^T\right) + u_k^2 p_{k_{KK}} bb^T + \Gamma Q\Gamma^T\right]^{-1}\right. \\
& - C^T\left\{CAP_{k_{xx}}A^TC^T + u_k\left[CAp_{k_{xK}}(Cb)^T + (Cb)\left(CAp_{k_{xK}}\right)^T\right]\right. \\
& \left.\left. + u_k^2 p_{k_{KK}}(Cb)(Cb)^T + C\Gamma Q\Gamma^T C^T + R\right\}^{-1} C\right\}^{-1}
\end{aligned}
$$

where we set

$$
\begin{aligned}
A_1 = {} & \left[AP_{k_{xx}}A^T + u_k\left(Ap_{k_{xK}}b^T + bp_{k_{xK}}^T A^T\right)\right. \\
& \left. + u_k^2 p_{k_{KK}} bb^T + \Gamma Q\Gamma^T\right]^{-1}
\end{aligned}
$$

$$A_2 = C^T$$

$$A_3 = C$$

$$
\begin{aligned}
A_4 = {} & \left\{CAP_{k_{xx}}A^TC^T + u_k\left[CAp_{k_{xK}}(Cb)^T + (Cb)\left(CAp_{k_{xK}}\right)^T\right]\right. \\
& \left. + u_k^2 p_{k_{KK}}(Cb)(Cb)^T + C\Gamma Q\Gamma^T C^T + R\right\}
\end{aligned}
$$

We obtain

$$
\begin{aligned}
& \left\{\left[AP_{k_{xx}}A^T + u_k\left(Ap_{k_{xK}}b^T + bp_{k_{xK}}^T A^T\right) + u_k^2 p_{k_{KK}} bb^T + \Gamma Q\Gamma^T\right]^{-1}\right. \\
& - C^T\left\{CAP_{k_{xx}}A^TC^T + u_k\left[CAp_{k_{xK}}(Cb)^T + (Cb)\left(CAp_{k_{xK}}\right)^T\right]\right. \\
& \left.\left. + u_k^2 p_{k_{KK}}(Cb)(Cb)^T + C\Gamma Q\Gamma^T C^T + R\right\}^{-1} C\right\}^{-1} \\
& = \left[AP_{k_{xx}}A^T + u_k\left(Ap_{k_{xK}}b^T + bp_{k_{xK}}^T A^T\right) + u_k^2 p_{k_{KK}} bb^T\right. \\
& \left. + \Gamma Q\Gamma^T\right] + \left[AP_{k_{xx}}A^T + u_k\left(Ap_{k_{xK}}b^T + bp_{k_{xK}}^T A^T\right)\right. \\
& \left. + u_k^2 p_{k_{KK}} bb^T + \Gamma Q\Gamma^T\right] C^T \times \left\{\left\{CAP_{k_{xx}}A^TC^T\right.\right. \\
& + u_k\left[CAp_{k_{xK}}(Cb)^T + (Cb)\left(CAp_{k_{xK}}\right)^T\right] \\
& \left. + u_k^2 p_{k_{KK}}(Cb)(Cb)^T + C\Gamma Q\Gamma^T C^T + R\right\} \\
& - C\left[AP_{k_{xx}}A^T + u_k\left(Ap_{k_{xK}}b^T + bp_{k_{xK}}^T A^T\right)\right. \\
& \left.\left. + u_k^2 p_{k_{KK}} bb^T + \Gamma Q\Gamma^T\right] C^T\right\}^{-1} \times C\left[AP_{k_{xx}}A^T\right. \\
& \left. + u_k\left(Ap_{k_{xK}}b^T + bp_{k_{xK}}^T A^T\right) + u_k^2 p_{k_{KK}} bb^T + \Gamma Q\Gamma^T\right]
\end{aligned}
$$

Reducing the preceding equation gives

$$
\begin{aligned}
& \left[AP_{k_{xx}}A^T + u_k\left(Ap_{k_{xK}}b^T + bp_{k_{xK}}^T A^T\right) + u_k^2 p_{k_{KK}} bb^T + \Gamma Q\Gamma^T\right] \\
& \times\left\{\left[AP_{k_{xx}}A^T + u_k\left(Ap_{k_{xK}}b^T + bp_{k_{xK}}^T A^T\right) + u_k^2 p_{k_{KK}} bb^T\right.\right. \\
& \left.\left. + \Gamma Q\Gamma^T\right]^{-1} + C^T R^{-1} C\right\} \times \left[AP_{k_{xx}}A^T\right. \\
& \left. + u_k\left(Ap_{k_{xK}}b^T + bp_{k_{xK}}^T A^T\right) + u_k^2 p_{k_{KK}} bb^T + \Gamma Q\Gamma^T\right]
\end{aligned}
$$

Hence, Eq. (A13) can now be reduced to

$$
\begin{aligned}
P_{k+1_{xx}} = {} & \left\{\left[AP_{k_{xx}}A^T + u_k\left(Ap_{k_{xK}}b^T + bp_{k_{xK}}^T A^T\right)\right.\right. \\
& \left.\left. + u_k^2 p_{k_{KK}} bb^T + \Gamma Q\Gamma^T\right]^{-1} + C^T R^{-1} C\right\}^{-1}
\end{aligned} \tag{A14}
$$

In addition,

$$
\begin{aligned}
p_{k+1_{KK}} = {} & p_{k_{KK}} - \left[\left(CAp_{k_{xK}}\right)^T + u_k p_{k_{KK}}(Cb)^T\right] \\
& \times\left\{CAP_{k_{xx}}A^TC^T + u_k\left[CAp_{k_{xK}}(Cb)^T + (Cb)\left(CAp_{k_{xK}}\right)^T\right]\right. \\
& \left. + u_k^2 p_{k_{KK}}(Cb)(Cb)^T + C\Gamma Q\Gamma^T C^T + R\right\}^{-1} \\
& \times\left(CAp_{k_{xK}} + u_k p_{k_{KK}} Cb\right)
\end{aligned} \tag{A15}
$$

$$
\begin{aligned}
p_{k+1_{xK}} = {} & Ap_{k_{xK}} + u_k p_{k_{KK}} b - \left\{AP_{k_{xx}}A^TC^T\right. \\
& + u_k\left[Ap_{k_{xK}}(Cb)^T + b\left(CAp_{k_{xK}}\right)^T\right] + u_k^2 p_{k_{KK}} b(Cb)^T \\
& \left. + \Gamma Q\Gamma^T C^T\right\}\left\{CAP_{k_{xx}}A^TC^T + u_k\left[CAp_{k_{xK}}(Cb)^T\right.\right. \\
& \left. + (Cb)\left(CAp_{k_{xK}}\right)^T\right] + u_k^2 p_{k_{KK}}(Cb)(Cb)^T \\
& \left. + C\Gamma Q\Gamma^T C^T + R\right\}^{-1}\left(CAp_{k_{xK}} + u_k p_{k_{KK}} Cb\right)
\end{aligned} \tag{A16}
$$

We also partition the Kalman gain vector as follows:

$$
K = \begin{pmatrix} K_x \\ K_K \end{pmatrix} \tag{A17}
$$

where

$$
\begin{aligned}
K_x = {} & \left\{AP_{k_{xx}}A^TC^T + u_k\left[Ap_{k_{xK}}(Cb)^T + b\left(CAp_{k_{xK}}\right)^T\right]\right. \\
& \left. + u_k^2 p_{k_{KK}} b(Cb)^T + \Gamma Q\Gamma^T C^T\right\} \times \left\{CAP_{k_{xx}}A^TC^T\right. \\
& + u_k\left[CAp_{k_{xK}}(Cb)^T + (Cb)\left(CAp_{k_{xK}}\right)^T\right] \\
& \left. + u_k^2 p_{k_{KK}}(Cb)(Cb)^T + C\Gamma Q\Gamma^T C^T + R\right\}^{-1}
\end{aligned} \tag{A18}
$$

$$K_K = \left[\left(CAp_{k_{xK}}\right)^T + u_k p_{k_{KK}}(Cb)^T\right] \times \left\{CAP_{k_{xx}}A^TC^T + u_k\left[CAp_{k_{xK}}(Cb)^T + (Cb)\left(CAp_{k_{xK}}\right)^T\right] + u_k^2 p_{k_{KK}}(Cb)(Cb)^T + C\Gamma Q\Gamma^T C^T + R\right\}^{-1} \quad \text{(A19)}$$

Hence, we finally obtain

$$\hat{x}_{k+1} = A\hat{x}_k + \hat{K}_k b u_k + K_x(z_{k+1} - CA\hat{x}_k - \hat{K}_k Cbu_k) \quad \text{(A20)}$$

$$\hat{K}_{k+1} = \hat{K}_k + K_K(z_{k+1} - CA\hat{x}_k - \hat{K}_k Cbu_k) \quad \text{(A21)}$$

□

Proposition: An additional application of the MIL will reduce the number of matrix inversions such that only the low-order matrix

$$CAP_{k_{xx}}A^TC^T + u_k\left[CAp_{k_{xK}}(Cb)^T + (Cb)\left(CAp_{k_{xK}}\right)^T\right] + u_k^2 p_{k_{KK}}(Cb)(Cb)^T + C\Gamma Q\Gamma^T C^T + R$$

needs to be inverted.

Corollary: Consider the classical Kalman filter paradigm where the loop gain K is known, that is, $K = 1$. In this special case

$$p_{0_{KK}} = 0, \qquad p_{0_{xK}} = 0, \qquad p_{k_{KK}} = 0, \qquad p_{k_{xK}} = 0 \quad \text{for all} \quad k = 1, 2, 3, \ldots \quad \text{(A22)}$$

and it follows that

$$P_k = P_{k_{xx}} \quad \text{(A23)}$$

$$K_K = 0 \quad \text{(A24)}$$

$$K_x = \left(AP_{k_{xx}}A^T + \Gamma Q\Gamma^T\right)C_T \times \left(CAP_{k_{xx}}A^TC^T + C\Gamma Q\Gamma^T C^T + R\right)^{-1} \quad \text{(A25)}$$

$$P_{k+1_{xx}} = \left[\left(AP_{k_{xx}}A^T + \Gamma Q\Gamma^T\right)^{-1} + C^T R^{-1} C\right]^{-1} \quad \text{(A26)}$$

Thus, the classical Kalman filter formulas are recovered. □

References

[1] Caglayan, A. K., "Detection, Identification and Estimation of Surface Damage/Actuator Failure for High Performance Aircraft," *Proceedings of the 7th American Control Conference*, Inst. of Electrical and Electronic Engineers, Piscataway, NJ, 1988, pp. 2206–2212.

[2] Maybeck, P., *Stochastic Models, Estimation and Control*, Vol. 3, 1st ed., Academic Press, San Diego, CA, 1994, pp. 247–255.

[3] Chandler, P., and Pachter, M., "Constrained Linear Regression for Flight Control System Failure Identification," *Proceedings of the American Control Conference*, Inst. of Electrical and Electronic Engineers, Piscataway, NJ, 1993, pp. 3141–3145.

[4] Chandler, P., and Pachter, M., "Regression Techniques for Aircraft Parameter Identification from Noisy Measurements in Maneuvering Flight," *Proceedings of the 31st Conference on Decision and Control*, Inst. of Electrical and Electronic Engineers, Piscataway, NJ, 1992, pp. 2311–2316.

[5] Chandler, P., Pachter, M., and Mears, M., "System Identification for Adaptive and Reconfigurable Control," *Journal of Guidance, Control, and Dynamics*, Vol. 18, No. 3, 1995, pp. 516–524.

[6] Pachter, M., and Sillence, J., "Loop Gain Identification for Adaptive and Reconfigurable Control," *Proceedings of the American Control Conference*, Inst. of Electrical and Electronic Engineers, Piscataway, NJ, 2000.

[7] Huang, Y.-S., "Adaptive and Reconfigurable Flight Control," Ph.D. Dissertation, Rept. AFIT/DS/ENG/01-02, School of Engineering and Management, U.S. Air Force Inst. of Technology, Wright–Patterson AFB, OH, March 2001.

[8] Maybeck, P., *Stochastic Models, Estimation and Control*, Vol. 1, 1st ed., Academic Press, San Diego, CA, 1994, p. 203.

[9] Blakelock, J. H., *Automatic Control of Aircraft and Missiles*, Wiley, New York, 1991, p. 46.

[10] Pachter, M., and Chandler, P., "Reconfigurable Tracking Control with Saturation," *Journal of Guidance, Control, and Dynamics*, Vol. 18, No. 5, 1995, pp. 1016–1022.